THE ASTROPHYSICAL JOURNAL, 376:8–22, 1991 July 20

THE DISTANCE TO THE COMA CLUSTER USING THE *B*-BAND TULLY-FISHER RELATION

M. FUKUGITA
Yukawa Institute for Theoretical Physics, Kyoto University, Kyoto 606, Japan

S. OKAMURA AND K. TARUSAWA
Kiso Observatory, Institute of Astronomy, University of Tokyo, Mitake-mura, Kiso-gun, Nagano 397-01, Japan

H. J. ROOD
Institute for Advanced Study, Princeton, NJ 08540

AND

B. A. WILLIAMS
Department of Physics, University of Delaware, Newark, DE 19716
Received 1990 August 13; accepted 1991 January 16

ABSTRACT

The distance to the Coma cluster was estimated using the *B*-band Tully-Fisher relation. We took all galaxies for which H I line width data are available in a circle of 4° radius centered on the Coma cluster, and carried out photographic surface photometry on them. The sample represents a substantial fraction of all spiral galaxies for $m_z < 15.5$ mag inside this circle. We estimated carefully possible errors which would enter in each step to form the Tully-Fisher relation. In particular, a detailed estimate was made of the cluster population incompleteness bias for the distance estimation. We found that the correction for the sample incompleteness, when combined with the dispersion of the Tully-Fisher relation, increases the distance modulus by 0.3 mag, but that it cannot be as large as the value recently suspected by Kraan-Kortweg, Cameron and Tammann. As our best estimate for the Coma cluster we obtained the distance modulus of $(m - M)^0 = 34.5 \pm 0.4$, which corresponds to a Hubble constant $H_0 = 92^{+21}_{-17}$ km s^{-1} Mpc^{-1}.

Subject headings: cosmology — galaxies: clustering — galaxies: distances — galaxies: photometry — radio sources: 21 cm radiation

1. INTRODUCTION

Since the discovery of a relationship between the luminosity of a spiral galaxy and H I 21 cm line width (Tully & Fisher 1977), a large amount of effort has been invested in estimating the extragalactic distances with the use of this Tully-Fisher relation (hereafter TF relation) applied to various optical bands (e.g., Sandage & Tammann 1976, 1984; Aaronson, Huchra, & Mould 1979; Bottinelli et al. 1983; Richter & Huchtmeier 1984; Aaronson et al. 1986, hereafter ABMHSC; Pierce & Tully 1988; Tully 1988; Kraan-Korteweg, Cameron, & Tammann 1988, hereafter KCT; Sandage 1988; Fouqué et al. 1990). While the use of the TF relation is believed to have brought substantial progress in the art of estimating extragalactic distances, an inherent controversy still remains over the value of the Hubble constant. Its measured variation between different observers is much larger than their claimed internal uncertainties.

The traditional first step to the Hubble constant program is the determination of the distance to the Virgo cluster. The use of the Virgo cluster for this purpose, however, has serious limitations in that there exists an inherently large uncertainty in the correction for the infall velocity of the Local Group (LG) towards the Virgo cluster which is model-dependent (e.g., Davis & Peebles 1983), as well as a significant uncertainty in the estimate of the average recession velocity, which depends on the choice of the sample (Arp 1988; see, e.g., de Vaucouleurs 1982; Tammann & Sandage 1985; Huchra 1985). In this respect, it is highly desirable to use clusters beyond Virgo especially to reduce uncertainties associated with peculiar velocities. On the other hand, the numbers of galaxy samples beyond the Virgo cluster that are available for the TF analysis usually contain in the order of 10 or so galaxies per cluster. The paucity of sample galaxies then leaves the suspicion that the sample may suffer from a strong selection effect towards brighter galaxies (e.g., Tammann, Sandage, & Yahil 1980; Teerikorpi 1987; Bottinelli et al. 1987; Feast 1987; Sandage 1988; KCT). The problem is that the samples were not selected optically, but selected according to the availability of the H I line width data. In fact, KCT suggested that this bias is the source of the smaller distance modulus of clusters and proposed an "upper envelope prescription" to correct for this bias, which leads to distance moduli ~1 mag larger than the value obtained from the standard procedure. We expect that we can clarify this issue using if not a complete magnitude-limited sample for clusters, at least a sample for which the completeness is under control. We also note that, in general, the photometry data may not be quite sufficient (with an exception of the recent study by Pierce & Tully 1988 for the nearby cluster of Ursa Major) to evaluate the total magnitude which is needed to form the TF relation; for instance the *B*-band total magnitude by Bothun et al. (1985, hereafter BASMHS), which has been widely adopted for the TF relation analyses for distant clusters, is based on photometry with single or few apertures.

In this paper we try to study the problems for the Coma cluster using the TF relation in the *B* band by carefully examining possible sources of errors and biases in the step to construct the TF relation. Previous work on the application of the TF relation to the Coma cluster includes Aaronson et al. (1980, 1986), Bottinelli et al. (1987), and KCT. The sample sizes used by these authors are 13, 24, and 13. The paucity of available sample galaxies comes from the fact that this relatively spiral-poor cluster is located almost at the limiting distance obtainable with presently available H I techniques. In our analysis we apply all available H I data for the galaxies located within a circle of radius 4° (more precisely 260′ circle) from the Coma cluster center (defined here to be at NGC 4889) published in the literature (32 galaxies) and previously unpublished new data (18 galaxies) obtained by Williams & Rood (1988). They attempted to measure the H I line width of all spiral candidates brighter than Zwicky apparent magnitude $m_z = 15.7$ mag according to the Catalogue of Galaxies and of Cluster of Galaxies (Zwicky et al. 1961–1968, hereafter CGCG) in a 4° radius centered on the Coma cluster. We consider the 4° radius optimum for our purpose, because there is little uncertainty as to cluster membership out to this radius (Kent & Gunn 1982), and the H I sample completeness turns out to be reasonably good to this radius. We then made surface photometry using Schmidt plates for all galaxies, obtaining accurate and homogeneous magnitude data. At the same time inclinations, which are major sources leading to uncertainty in the distance estimate based on the TF relation, were measured from the plates.

We followed the standard procedure and kept corrections and sample selections to a minimum to avoid extra model dependences which might come in with elaborate procedures often taken by a few authors. In particular, we assumed the TF relation to be linear. We tried to make a careful estimate of uncertainties and model dependences caused by each step of the measurement and the correction procedures. Particular attention was paid to the estimate of the effect of cluster population incompleteness on the distance determination.

An additional merit in studying the Coma cluster as a distance estimator is its direction which is almost perpendicular to that of the alleged large-scale streaming motion (Dressler et al. 1987a). The cluster would not suffer from this effect even if a region out to $\approx 70h^{-1}$ Mpc distance is participating in such a motion; hence the Coma cluster is a good object to determine the universal expansion parameter.

The outline of the paper is as follows. In § 2 we present a compilation of H I line width data and estimate the completeness of the H I sample. The surface photometry results are described in this section, and they are compared with the existing photometry data. We then estimate absorption corrections and discuss their model dependences. The TF relation is given in § 3 both for local calibrators and for Coma cluster galaxies with detailed discussion of uncertainties in the distance estimate. The bias caused by cluster population incompleteness is also estimated in this section. In § 4 we repeat the TF analysis with a reduced-size sample to facilitate a comparison with the previous analyses in the literature, and a brief comment is given on them. Finally our conclusion is summarized in § 5.

2. DATA

2.1. H I *Line Width Data*

The H I data are taken from BASMHS for 27 galaxies and from Chincarini, Giovanelli, & Haynes (1983) for 21 galaxies within the circle of 260′ radius from the center of the Coma cluster. Among them 16 galaxies have measurements from both sources. Williams & Rood (1988) attempted to measure the H I line width for 79 galaxies in a circle of radius slightly larger than 4° from the Coma center using the 305 m telescope at Arecibo, and yielded good line widths for 18 galaxies. Of them, two have already published widths. We have a total of 48 galaxies with good line width data, which are summarized in Table 1. Their spatial distribution on the sky is shown in Figure 1. All of these galaxies except for three are cataloged in CGCG.

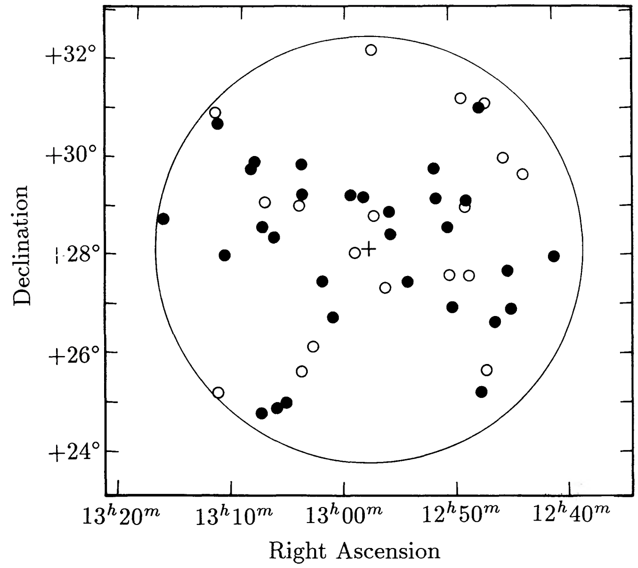

FIG. 1.—Spatial distribution of 48 galaxies with the H I line width data. Solid points represent the 30 galaxies which are used to form the TF relation. The cross stands for the center of the Coma cluster (defined to be at NGC 4889) and the circle represents 260′ angular radius from the center.

We use the line width at 20% of the line-profile peak values throughout the present analysis. The quoted rms error of the line width is typically ± 20 km s^{-1} for a good measurement, but it may amount to ± 50 km s^{-1} for poorly measured galaxies. For the line width data of Chincarini et al. (1983) we added 8 km s^{-1} according to the prescription given by Haynes & Giovanelli (1984), in order to translate their tabulated data, which represent the average of the line width at 20% of the peak and that at 50% of the average flux, into the 20% line width. We compared the corrected data against those by BASMHS for 18 galaxies common to both samples (2 outside the 260′ circle), and found that there is no relative systematic zero point error; $\Delta v(\text{CGH}) = \Delta v(\text{BASMHS}) - 0.9$ km s^{-1}. The dispersion between the two sets of data is 35 km s^{-1}. We adopt the average value for our analysis when two (or three) measurements are available. The signal-to-noise ratio of the new data by Williams & Rood (1988) mostly satisfies $S/N \gtrsim 6$, except for NGC 4735, the S/N of which is 3.1.[1]

Let us consider the problem of sample completeness. In Figure 2*a* we show histograms in m_z for 282 galaxies listed in CGCG (alleged to be nominally complete to $m_z = 15.5$ mag) in the 260′ circle from the center and of 48 galaxies in our sample. Histograms shown in Figure 2*b* are for the 93 galaxies with $m_z < 17$ mag in the Uppsala General Catalogue of Galaxies (Nilson 1973, hereafter UGC) within the same circle and a hatched part (54 galaxies) representing those classified as spirals (including S0/a). The UGC is supposed to be nominally complete down to $m_z = 14.5$ mag, and this in fact is justified by

[1] This small S/N would cause a bias towards a smaller line width, if we accept the result of a Monte Carlo simulation of Lewis (1983). We include this galaxy in our sample, since the data do not seem singular in the final TF plot, keeping in mind the possibility for some underestimate of its line width, however.

TABLE 1

Galaxies with H i Line Width Data in the 260′ Circle from the Coma Center

ID Number (1)	IC/NGC (2)	UGC (3)	CGCG[a] (4)	$V_\odot$ (km s^{-1}) (5)	Δv (km s^{-1}) Value (6)	Reference (7)	m_z (8)	B_T (9)	$a \times b$ (10)
1	I821	U7957	Z159076	6740	253	(1)	14.5	14.19	1′22 × 1′04
					239	(2)			
2	I826		Z159095	6937	223	(2)	14.9	14.71	0.83 × 0.63
3	I842	U8118	Z160088	7275	406	(1)	14.6	14.45	1.25 × 0.63
					394	(2)			
					435	(3)			
4	I854		Z130014	7085	287	(3)	15.1	14.74	1.01 × 0.59
5	I3913		Z160026	7534	225	(1)	15.5	15.20	0.82 × 0.52
6	I4088	U8140	Z160102	7104	496	(1)	14.8	14.65	1.69 × 0.52
					518	(2)			
7	I4202	U8220	Z130012	7122	568	(3)	15.2	14.85	1.88 × 0.38
8	I4210		Z160155	6375	263	(3)	15.3	14.86	0.90 × 0.61
9	N4712	U7977	Z129025	4382	404	(1)	13.5	13.40	2.47 × 1.01
10	N4735		Z159091	6402	335	(3)	15.1	14.93	0.70 × 0.47
11	N4738	U7999	Z159092	4765	471	(1)	14.9	14.62	2.05 × 0.40
12	N4848	U8082	Z160055	6991	487	(2)	14.2	14.25	1.36 × 0.49
13	N4921	U8134	Z160095	5450	168	(1)	13.7	13.20	2.26 × 1.95
					208	(2)			
14	N4966	U8194	Z160137	7035	456	(1)	13.9	13.99	1.27 × 0.70
					414	(2)			
15	N4979	U8209	Z130009	6326	256	(3)	15.3	14.27	1.39 × 0.83
16	N5000	U8241	Z160152	5613	215	(1)	14.0	13.71	1.67 × 1.29
					171	(2)			
17	N5032	U8300	Z160166	6408	563	(2)	13.6	13.71	2.02 × 1.10
18	N5041	U8319	Z160168	7477	308	(1)	14.2	13.89	1.63 × 1.29
					303	(2)			
19	N5081	U8366	Z160192	6655	569	(1)	14.3	13.77	2.16 × 0.80
					579	(2)			
20		U7890	Z159059	7528	294	(2)	14.5	14.80	0.73 × 0.52
21		U7955		6751	419	(3)	16.0	15.40	1.39 × 0.31
22		U7978	Z159082	8086	339	(1)	14.8	14.57	1.15 × 0.66
					341	(2)			
23		U8013	Z159099	7885	396	(1)	15.7	15.09	1.44 × 0.42
24		U8017	Z159102	7072	562	(1)	14.5	14.35	1.11 × 0.47
					660	(2)			
25		U8025	Z159110	6316	536	(2)	14.8	14.54	2.02 × 0.38
26		U8161	Z160121	6644	396	(1)	15.5	15.11	1.43 × 0.52
					385	(2)			
27		U8195		7043	266	(1)	16.0	15.49	1.32 × 0.28
28		U8229	Z160148	5967	421	(1)	14.3	14.17	1.32 × 0.87
					372	(2)			
29		U8244		7100	312	(1)	16.0	15.24	1.25 × 0.52
					297	(2)			
30		U8259	Z160156	7284	400	(3)	15.3	14.60	1.36 × 0.63
31		U8317	Z160167	6035	307	(3)	15.0	14.57	1.15 × 0.49
32			Z129026	6465	224	(3)	15.4	15.34	0.87 × 0.49
33			Z130006	6512	218	(3)	15.0	14.75	0.73 × 0.59
34			Z130008	7267	246	(1)	14.9	14.85	0.64 × 0.47
					231	(2)			
35			Z130021	7246	300	(3)	15.4	14.81	0.97 × 0.73
36			Z159071	6970	275	(3)	15.5	15.84	0.87 × 0.63
37			Z159075	6647	344	(3)	15.2	15.08	0.76 × 0.43
38			Z159080	6881	377	(3)	15.7	15.26	0.89 × 0.37
39			Z159081	8111	184	(3)	15.5	15.49	0.73 × 0.56
40			Z159090	8317	155	(1)	15.5	15.20	0.97 × 0.49
41			Z159101	7745	180	(1)	15.3	15.60	0.52 × 0.43
42			Z159106	7947	346	(3)	15.6	15.58	0.73 × 0.35
43			Z160058	7653	377	(1)	15.5	15.03	1.04 × 0.42
					334	(3)			
44			Z160067	7659	241	(1)	15.4	15.52	0.50 × 0.37
45			Z160076	5345	100	(1)	15.6	15.52	0.59 × 0.52
					140	(2)			
46			Z160080	6822	137	(1)	14.7	14.65	0.96 × 0.76
					130	(2)			
47			Z160127	5523	209	(1)	15.5	15.29	0.80 × 0.52
48			Z160139	4761	219	(1)	15.0	14.77	1.08 × 0.57

Notes.—Col. (5) heliocentric velocity taken from the compilation by Huchtmeier et al. 1983. Col. (6) H i 21 cm line width at 20% of the peak. Col. (7) References: (1) BASMHS; (2) Chincarini, Giovanelli, & Haynes 1983, 8 km s^{-1} is added according to Haynes & Giovanelli 1984; (3) Williams & Rood 1988. Col. (8) Zwicky magnitude as tabulated in CGCG. Col. (9) total magnitude measured in the present study. Col. (10) major and minor axes at $\mu = 25$ mag arcsec^{-2} measured in the present study.

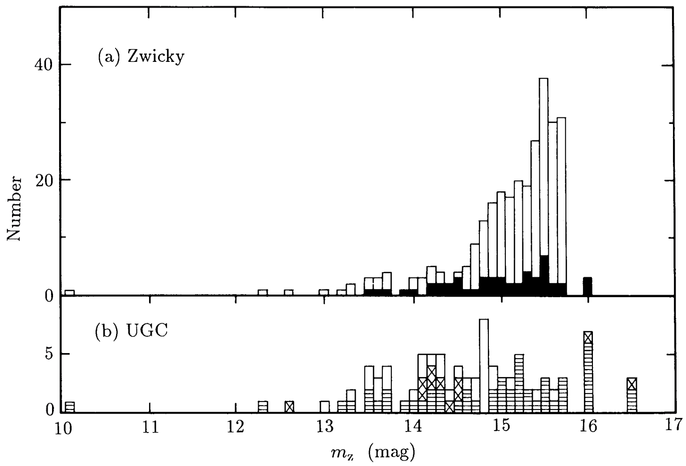

FIG. 2.—(*a*) Histograms of galaxies in the circle of 260′ radius as a function of the Zwicky magnitude listed in CGCG and those in our sample (*black part*). (*b*) Histogram of UGC galaxies in the circle of 260′ radius (3 galaxies with $m_z \geq 17$ mag are not shown). The hatched part (54 galaxies) shows spirals and crossed part indicates galaxies with unknown morphologies (spiral candidates).

comparing the histogram for UGC with that for CGCG. By comparing our sample (Fig. 2*a*) with spirals in UGC (Fig. 2*b*) in the interval from 13 to 14.5 mag, we see that the completeness of our sample is more than 80% down to 14.5 mag. For $m_z > 14.5$ mag we infer the completeness in the following way: From the histograms for $m_z < 14.5$ mag we estimate the spiral fraction to be about 40%–45%.[2] If we assume that the luminosity function is universal irrespective of morphological type down to $M_z \sim -18.7$ mag, we expect 24–27 spirals in the range of 14.5–15 mag and 48–55 for 15–15.5 mag. In these magnitude ranges our sample contains 11 and 18 galaxies, respectively, and the completeness is estimated to be ~45% for the former and ~35% for the latter (see Fig. 3). Beyond 15.5 mag the completeness of our sample drops sharply. This analysis shows that the sample that we work with represents a substantial fraction of spiral galaxies down to 15.5 mag. The effect of sample incompleteness bias on the distance estimation will be discussed in § 3.3.

2.2. *Surface Photometry*

We have exposed, with extensive overlaps, five 6° × 6° Schmidt plates in the *B* band (Kodak IIa-O emulsion plus Schott GG385 filter) on a 10° × 10° region centered on the Coma cluster using the 105 cm Schmidt telescope at the Kiso

[2] This is compared with the estimate by Rood et al. (1972), who reported that about 18% are spiral galaxies in the 245′ circle. We note that our sample is contaminated by foreground galaxies and the true fraction for the Coma members is a little smaller than we estimated.

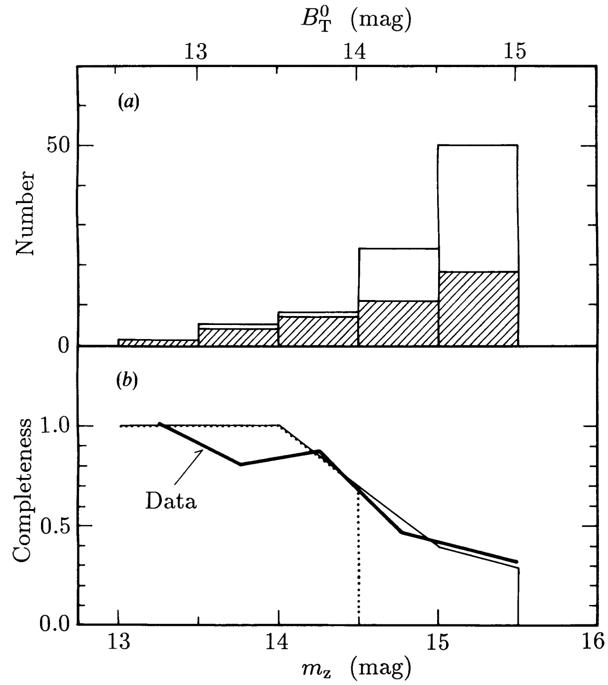

FIG. 3.—(*a*) Histograms of estimated spiral galaxies in the circle of 260′ radius compared with those in our sample (*hatched part*). (*b*) The estimated completeness of the sample. Two additional curves (denoted by thin line and dotted line) are selection functions used in § 4.

Observatory. The log of the plates is given in Table 2. The plates were scanned with a PDS 2020GMS microdensitometer with a 17 μm aperture and a 10 μm (0″.625) sampling pitch. The standard surface photometry (e.g., Okamura 1988) was carried out for the relevant galaxies. Because of the plate overlap, 31 galaxies were exposed on two plates, six on three plates, one on four plates, and one on five plates. These galaxies were used to evaluate the internal error of the present photometry. In addition to the relevant spiral galaxies, nine early-type galaxies in the central region of the Coma cluster were measured for calibration of the zero point. In total, 114 frames for 57 galaxies were subjected to surface photometry. The size of the frame was 256 × 256 pixels (160″ square) except for a few large galaxies (NGC 4712, UGC 8025, NGC 4921, and NGC 5081), for which larger frames were secured.

To determine the zero point, the photoelectric aperture magnitudes (128 data points for four spiral and nine early-type galaxies) were taken from the compilation by Longo & de Vaucouleurs (1983). They were fitted by the least-squares method to the growth curve, i.e., the plot of the integrated magnitude as a function of aperture of the integration circle centered on a galaxy. The sky brightness determined from

TABLE 2

LOG OF THE PLATES

Plate Number	Plate Center (1950) α	Plate Center (1950) δ	Observation Date	Sky Brightness (mag arcsec^{-2})
K6147	$12^h57^m.5$	+28°15′	1989 Mar 8	22.28
K6146	12 47 0	+26 00	1989 Mar 8	22.30
K6145	13 07 0	+26 00	1989 Mar 8	22.25
K6144	12 47 0	+30 30	1989 Mar 8	22.01
K6110	13 07 0	+30 30	1989 Feb 6	21.99

these calibrators agrees within 0.08 mag (1 σ) for a single plate and it varies from 22.0 to 22.3 mag arcsec^{-2} from plate to plate. The difference between the sky brightness determined using the four spiral galaxies and that using the nine early-type galaxies is less than 0.08 mag. No systematic dependence of the sky brightness has been found on the position of calibrating galaxies on the plate.

Good isophotes were obtained down to the surface brightness $\mu_B = 25$ mag arcsec^{-2} with a moderate smoothing procedure. A growth curve was constructed from each of the smoothed frames with the abscissa (aperture) expressed in logarithmic units for convenience in a sliding fit. According to the standard procedure (e.g., de Vaucouleurs & Corwin 1977), a template was fitted to the individual growth curve. For consistency of photometry, we used a set of template growth curves presented numerically by de Vaucouleurs (1977), which is the same as shown in The Second Reference Catalogue of Bright Galaxies (de Vaoucouleurs, de Vaoucouleurs, & Corwin 1976, hereafter RC2). For early-type galaxies, templates for $T = 5$ or -3 were used and for spiral galaxies those for $T = 5$ or 7 were used, where T is the morphological type index given in RC2. Fitting was done graphically by sliding the template along both coordinate axes, and the total (asymptotic) magnitude, B_T, and the effective radius were read on the graph, although the latter parameter is not shown here. Since the present photometry is based on Schmidt plates on a small image scale (62″.5 mm^{-1}), the data in the very central fraction of a galaxy might not be reliable because of various photographic adjacency effects and finite seeing (Okamura 1988). Accordingly, the very central region [$\log A/D(0) \lesssim -0.5$] was not used in the fitting, although most galaxies are faint enough so that the saturation effect need not be cared for. The faint outer region [$\log A/D(0) \gtrsim 0.5$] was also assigned a lower weight to avoid the effects of noise and a possible slight error in the sky subtraction. The error in B_T estimated from data of the same galaxy derived from different plates is 0.016 mag, and the error arising from the sliding fit procedure is estimated to be 0.04 mag.

The external error was investigated by comparing our magnitudes with those in the literature. First, we made a comparison between our B_T(Kiso) and those listed in RC2 for 12 galaxies (two spirals and 10 early-type galaxies). We found $B_T(\mathrm{RC2}) = B_T(\mathrm{Kiso}) - 0.03$ with a dispersion of $\sigma = 0.16$ mag; no significant discrepancy was detected in the magnitude range 12.5–16 mag for both elliptical and spiral galaxies (Fig. 4*a*).

The most systematic photometry of spiral galaxies in the Coma cluster available to date is the aperture magnitudes by BASMHS. There are 35 aperture magnitudes in BASMHS for 26 galaxies in common with our sample. In order to make a comparison, integrated magnitudes were obtained from our photographic data within the BASMHS apertures for all of the common galaxies. Since we dealt with the data from different plates as independent data, there were 87 magnitudes available for the comparison, which is shown in Figure 4*b*. No conspicuous nonlinearity was detected over the entire range of magnitude where data are available.[3] We found, however, a zero point difference of 0.13 mag with our magnitude brighter and a dispersion of 0.11 mag. In order to examine the possibility that the saturation effect in the central region of a galaxy combined with an error of the characteristic curve could cause this zero point offset, we studied the magnitude difference between BASMHS and the present photometry as a function of the aperture size, the surface brightness within the aperture, and the aperture magnitude. No systematic trend was found, however, which hinted the saturation or error in the characteristic curve. (In fact, we have well-defined characteristic curves up to 5.11*D*, i.e., the full scale of the PDS microdensitometer while the highest density of the pixel in the nuclear region of the two brightest ellipticals is below 4.0*D* on all of the plates.) Another comparison was made with the aperture magnitudes from CCD photometry by Cornell et al. (1987) for seven common galaxies. This comparison of 18 magnitudes also showed a similar zero point difference of 0.175 mag with our magnitude brighter (Fig. 4*b*). Apart from this zero point offset, the agreement between the two magnitudes is quite satisfactory ($\sigma = 0.068$ mag). We conclude that our photographic photometry sustains a sufficient accuracy except for a possible slight error in the zero point (in a disagreement of the order of 0.13–0.17 mag between the photoelectric photometry data given in the Longo & de Vaoucouleurs 1984 compilation and those by BASMHS and by Cornell et al. 1987. Since the cause of this difference is not clear, we treat it provisionally as a possible systematic bias to our result).

Finally, in order to compare the total magnitudes of BASMHS with ours, we deduced B_T of BASMHS photometry from B_T^0 tabulated in Table 8 of their paper as $B_T = B_T^0 + 0.2(\sec i - 1) + 0.05$. The comparison for 25 common galaxies is shown in Figure 4*c*. We found that $B_T(\mathrm{BASMHS}) = B_T(\mathrm{Kiso}) + 0.23$ with $\sigma = 0.24$ on the average. The disagreement is particularly noticeable for faint galaxies. When we divide the sample into two at $B_T(\mathrm{BASMHS}) = 15$ mag, the offset (1 σ dispersion) is 0.11 mag (0.17 mag) for the brighter sample and 0.38 mag (0.24 mag) for the fainter sample, respectively. The discrepancy is sometimes as much as more than 0.5 mag for some low surface brightness galaxies (e.g., UGC 8244, UGC 8013). The difference for the brighter sample is consistent with the zero point offset for aperture magnitudes discussed above. A part of the larger offset for the faint sample may be due to the fact that BASMHS used a common growth curve for all the galaxies as well as to the errors in aperture magnitude for faint galaxies somewhat enhanced by the growth curve fitting procedure. We also note that most (70%) of the B_T by BASMHS are based on a magnitude using a single aperture.

Our B_T magnitude is tabulated in Table 1 together with the Zwicky magnitude given in CGCG. A comparison of these two magnitudes is given in Figure 4*d*, which shows that our B_T is brighter than m_z by 0.19 mag with a dispersion of 0.28 mag.

A measurement was also made of the major- and minor-axis angular diameters from our faintest isophote of $\mu = 25$ mag arcsec^{-2}. The results are tabulated in Table 1. The error of the estimate for the ratio $R_{25} = b/a$ is at most 10%. We also compare our b/a with that in UGC, which has been adopted in most of the TF analyses to date. The dispersion of our b/a relative to that of UGC is estimated to be about 10%, but it increases substantially for $i < 50°$ (see Fig. 5).

2.3. *Corrections*

To evaluate the TF relation a number of corrections are needed both for the line width data and for the magnitude data. We estimate the inclinations i of the spiral galaxies from a and b given in Table 1. We adopted the conventional formula

[3] At a more detailed level, magnitudes fainter than 15.2 mag have a larger dispersion. This might reflect difficulties in aperture photometry for very faint galaxies, as already noted in BASMHS.

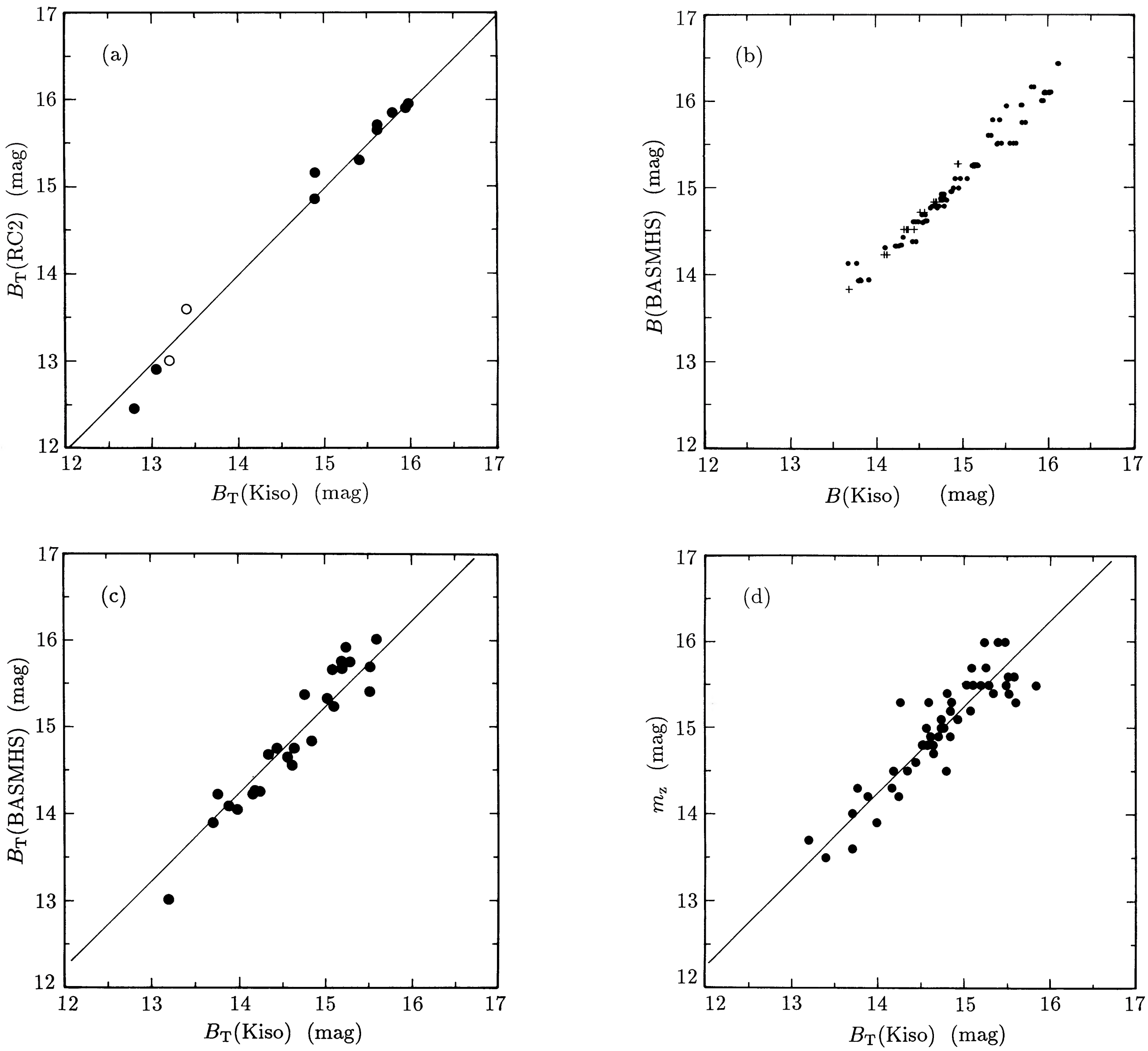

FIG. 4.—(*a*) Comparison of our B_T(Kiso) with those given in RC2 (cf. RC2). Spiral galaxies are shown by open circles and early-type galaxies by filled circles. The regression lines represents $B_T(\mathrm{RC2}) = B_T(\mathrm{Kiso}) - 0.03$. (*b*) Comparison of the aperture magnitudes between BASMHS (*dots*) and our photometry. The data by Cornell et al. (1987) (*crosses*) are also included. The data for the same galaxy from different plates are plotted as the independent data. (*c*) Comparison of B_T between BASMHS and our photometry. The regression line represents $B_T(\mathrm{BASMHS}) = B_T(\mathrm{Kiso}) + 0.23$. (*d*) Zwicky magnitude (m_z) vs. the total magnitude (B_T) for the 48 galaxies obtained by the present surface photometry.

given by Hubble (1926)

$$\cos^2 i = \frac{q^2 - q_0^2}{1 - q_0^2}, \tag{1}$$

with $q = b/a$ and q_0 fixed to 0.20. The use of a few alternatives to this formula is discussed in the literature (e.g., Aaronson, Mould, & Huchra 1980; Bottinelli et al. 1983). These alternatives, however, result in at most a 5% difference in $(\sin i)^{-1}$ for $i > 45°$, and this model-dependence is substantially smaller than the uncertainty in the estimate of b/a itself. A 10% uncertainty in b/a would result in a 11% uncertainty in $(\sin i)^{-1}$ for $i = 45°$, and it amounts to as much as 26% for $i = 35°$. We expect that the error in b/a is substantially smaller than 10% in our measurements. A caution should be made about this point when one uses b/a listed in the UGC catalog, however.

We convert the measured 21 profile width to an edge-on value using the simplest prescription as adopted by ABMHSC and KCT,

$$\Delta v^c = \frac{\Delta v}{\sin i(1 + z)}, \tag{2}$$

with z the redshift of a galaxy. As noted earlier the 20% line width is adopted for Δv. We did not apply corrections for turbulent velocities, because such a correction is at best model-

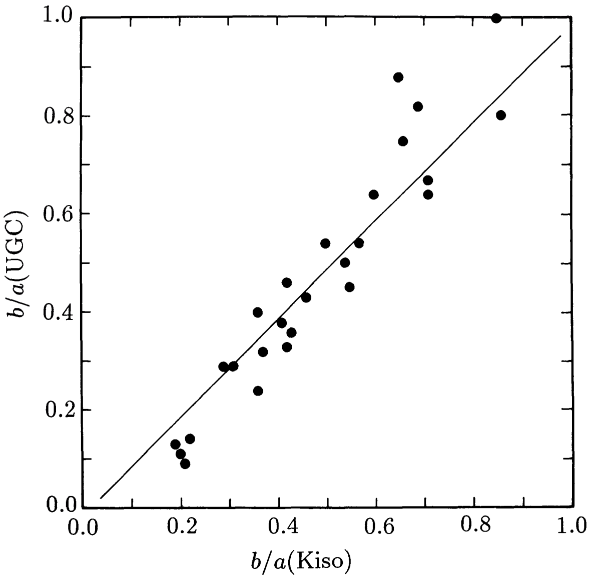

FIG. 5.—Axial ratios b/a in the UGC are compared with those obtained from the isophote of the present photometry at 25 mag arcsec^{-1}.

dependent.[4] We expect, however, that our neglect of this correction does not cause a significant problem in our case, since the reported turbulent velocities are of the order of $\lesssim 10$ km s^{-1} (van der Kruit & Shostak 1982; Lewis 1987) and most of the galaxies in our Coma sample have a velocity width larger than 250 km s^{-1}. Moreover, the correction was similarly omitted for the calibrating galaxies so that the error to the distance modulus caused by neglecting turbulent-motion correctons must be very small.

The corrected apparent total magnitude is given by

$$B_T^0 = B_T - A_B - A_i - K_B , \qquad (3)$$

where A_B is the Galactic extinction, A_i is the internal absorption, and K_B is the K-correction with $K_B = 0.03$–0.04 for spiral galaxies in the Coma cluster according to RC2. For A_B and A_i we attempted to use two alternative schemes widely employed in distance estimations, the corrections given in RC2 and that in A Revised Shapley-Ames Catalog of Bright Galaxies (Sandage & Tammann 1981, hereafter RSA) in a consistent manner. We also tried to estimate A_B with the scheme by Burstein & Heiles (1978, 1984, hereafter BH). For the Coma cluster $A_B = 0.19$ in the RC2 scheme, and $A_B = 0$ in RSA in approximate agreement with BH. The difference comes from the discrepancy in the polar cap reddening as discussed in BH. For the internal absorption the RSA scheme gives a larger absorption correction and A_i could differ by as much as 0.7 mag for early-type (Sa–Sb) spirals. On average we find $\langle A_i \rangle =$ 0.23 in RC2 and $\langle A_i \rangle = 0.59$ in RSA for 48 galaxies of our sample. We describe the corrected magnitudes for the RC2 and RSA scheme as B_T^0 and $B_T^{0,i}$ respectively.[5] The morphology data are taken from UGC and galaxies designated by " S " or of unknown morphologies are assumed to be Sb–Sc. The data used for the TF relation are given in Table 3.

[4] The correction by Bottinelli et al. (1983) amounts to 45–55 km s^{-1} for $i > 45°$, while Richter & Huchtmeier (1984) made a rather modest correction of 18 km s^{-1}. The correction with a more sophisticated form was proposed by Tully & Fouqué (1985).

[5] We note that the B_T^0 scheme used by BASMHS differs from the RC2 scheme adopted here. BASMHS used $A_B = 0$ instead of $A_B = 0.19$ in RC2, and $A_i = 0.2(\sec i - 1)$ rather than $\alpha \log R_{25}$ in RC2.

3. TULLY-FISHER RELATIONS

3.1. *Local Distance Calibrators*

Tammann (1987) has given a review of distance moduli to local calibrating galaxies. Since then there appeared several new studies on the distance moduli to nearby galaxies, including extensive work using infrared and/or multicolor photometry for Cepheid variables (Welch et al. 1986; Madore et al. 1987; Visvanathan 1989; Freedman 1990).

In the present work we adopt primarily the distance to the eight local calibrating galaxies (designated in Table 4) given by Tammann (1987) and KCT. It has been customary to derive the calibration curve by the least-square minimization procedure with an equal weight assigned to all distance data. We have to note, however, that only four calibrators (M31, M33, NGC 300 and NGC 2403) have the well measured distance by Cepheid variables and the distances to other calibrators are not as reliable as for these four. The distance to NGC 3031 (M81), which was revised as much as 1.1 mag from 1974 to 1987 (Tammann 1987), is now given the original 1974 value by Freedman (1990) and Jacoby et al. (1989). The distance to NGC 247, 253, and 7703 are estimated only through resolution into bright stars (Sandage & Tammann 1984). We, therefore, attempted to carry out the chi-square minimization with an appropriate weight put on these data. We estimate the weight from the scatter of the reported distance moduli including those that appeared after Tammann's (1987) review, with the central values, however, fixed on his original assignments. (We note that the distances reported by different investigators mostly fall within the range of errors shown here.) The weights we used are given in Column (7) of Table 4, and include the errors of photometry as given in RC2. For the three calibrators without Cepheids distance (NGC 247, 253, 7703), we assigned an error of 1.0 mag.

Attempts have often been made to increase the number of calibrators by assuming that several galaxies belong to the same group and therefore have the same distance; e.g., by assuming that NGC 2366, IC 2574 and NGC 4236 belong to the NGC 2403 group and NGC 5204, NGC 5585 to the M101 group with a distance modulus of 29.2 mag (KCT). We also tried to use this prescription, but in this case we reduced the weight for the relevant galaxies by the square root of the numbers of galaxies to avoid an unwanted overweight caused by the increase of the number of galaxies that belong to the same group, since the distance comes from only a single galaxy among them (Col. [8] of Table 4). Furthermore, with this prescription we can avoid overweighting fainter galaxies with log $\Delta v^c < 2.4$, which amount to more than one-half by number among the local calibrators when the number of calibrators is increased in this way. While the fitted curve is constrained rather strongly by the four calibrators with rather large line widths (log $\Delta v^c \gtrsim 2.4$), a consistent overall fit is also attained by including the fainter calibrators. We consider this procedure particularly suitable for our purpose, since we deal with galaxies with log $\Delta v^c \gtrsim 2.4$ in the Coma cluster.

The photometry data are basically taken from RC2 ($B_T^{0,i}$ is taken from KCT) and the line width data from Aaronson et al. (1982) except for NGC 300, for which the line width is not given by them. For this galaxy we use the line width by Rogstad, Crutcher, & Chu (1979). The coefficients of the fit

TABLE 3

Data for the Tully-Fisher Relation

ID Number (1)	Galaxy ID (2)	i (3)	Δv^c (km s^{-1}) (4)	B_T^0 (5)	$B_T^{0,i}$ (6)	Rejection (7)
1	I821	32	452	13.90	13.81	$i < 45°$
2	I826	42	328	14.38	14.28	$i < 45°$
3	I842	62	456	13.98	13.87	
4	I854	56	339	14.31	14.21	
5	I3913	52	278	14.81	14.71	
6	I4088	76	510	14.01	13.49	
7	I4202	88	555	14.05	13.94	
8	I4210	49	343	14.49	14.39	
9	N4712	69	427	12.88	12.76	foreground
10	N4735	49	434	14.56	14.46	
11	N4738	90	464	13.83	13.72	foreground
12	N4848	72	500	13.67	13.19	
13	N4921	31	357	12.93	12.65	foreground
14	N4966	58	499	13.55	13.44	
15	N4979	55	306	13.86	13.76	
16	N5000	40	292	13.40	13.10	$i < 45°$
17	N5032	59	644	13.27	12.89	
18	N5041	39	479	13.58	13.48	$i < 45°$
19	N5081	71	592	13.19	12.72	
20	U7890	46	400	14.45	14.35	
21	U7955	84	412	14.65	14.51	
22	U7978	57	396	14.15	14.04	
23	U8013	78	395	14.43	14.30	
24	U8017	68	646	13.82	13.70	
25	U8025	90	525	13.74	13.18	
26	U8161	72	402	14.53	14.40	
27	U8195	86	261	14.72	14.58	
28	U8229	50	507	13.81	13.47	
29	U8244	68	321	14.71	14.58	
30	U8259	65	432	14.10	13.68	
31	U8317	67	326	14.05	13.93	
32	Z129026	58	260	14.91	14.80	
33	Z130006	37	355	14.44	14.35	$i < 45°$
34	Z130008	44	337	14.50	14.41	$i < 45°$
35	Z130021	42	436	14.47	14.38	$i < 45°$
36	Z159071	45	382	15.50	15.40	$i < 45°$
37	Z159075	57	400	14.65	14.54	
38	Z159080	68	397	14.73	14.60	
39	Z159081	41	274	15.17	15.07	$i < 45°$
40	Z159090	62	171	14.72	14.61	background
41	Z159101	35	306	15.30	15.21	$i < 45°$
42	Z159106	64	376	15.09	14.98	
43	Z160058	69	374	14.48	14.36	
44	Z160067	43	342	15.19	15.08	$i < 45°$
45	Z160076	29	245	15.26	15.16	foreground
46	Z160080	39	210	14.34	14.24	$i < 45°$
47	Z160127	51	264	14.92	14.82	
48	Z160139	60	249	14.33	14.22	foreground

TABLE 4

Local Calibrators of the Tully-Fisher Relation

Number (0)	Name (1)	B_T (2)	B_T^0 (3)	$B_T^{0,i}$ (4)	$(m - M)^0$ (5)	$\log \Delta v_c$ (6)	Inverse (7)	Weight (8)
1	NGC 224[a]	4.36	3.59	3.12	24.2	2.745	0.20	0.20
2	NGC 598[a]	6.26	5.79	5.69	24.4	2.403	0.30	0.30
3	NGC 300[a]	8.70	8.38	8.31	26.0	2.371	0.51	0.51
4	NGC 247[a]	9.4	8.85	8.88	26.8	2.362	1.01	1.01
5	NGC 253[a]	8.04	7.40	7.38	27.5	2.641	1.00	1.00
6	NGC 7793[a]	9.70	9.36	9.25	27.5	2.389	1.01	1.01
7	NGC 2403[a]	8.85	8.30	8.29	27.8	2.479	0.41	0.82
8	NGC 2366	11.40	10.67	11.03	27.8	2.100	...	0.82
9	IC 2574	11.03	10.45	10.69	27.8	2.140	...	0.83
10	NGC 4236	9.95	9.32	9.35	27.8	2.299	...	0.84
11	NGC 3031[a]	7.75	7.24	7.01	28.7	2.725	1.10	1.10
12	NGC 5204	11.75	11.33	11.29	29.2	2.190	...	1.74
13	NGC 5585	11.4	11.02	10.94	29.2	2.318	...	1.74
14	Ho IV	13.10	12.46	12.76	29.2	2.033	...	1.74

[a] Direct distance determination is available.

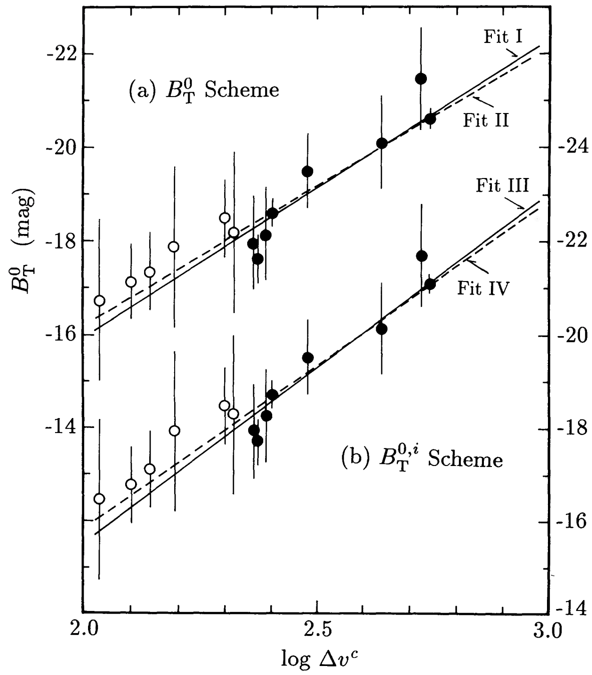

FIG. 6.—(*a*) TF relation for local calibrators. Solid points represent eight key calibrators described in the text. The B_T^0 scheme of RC2 is adopted. (*b*) Same as (*a*) with the $B_T^{0,i}$ scheme of RSA.

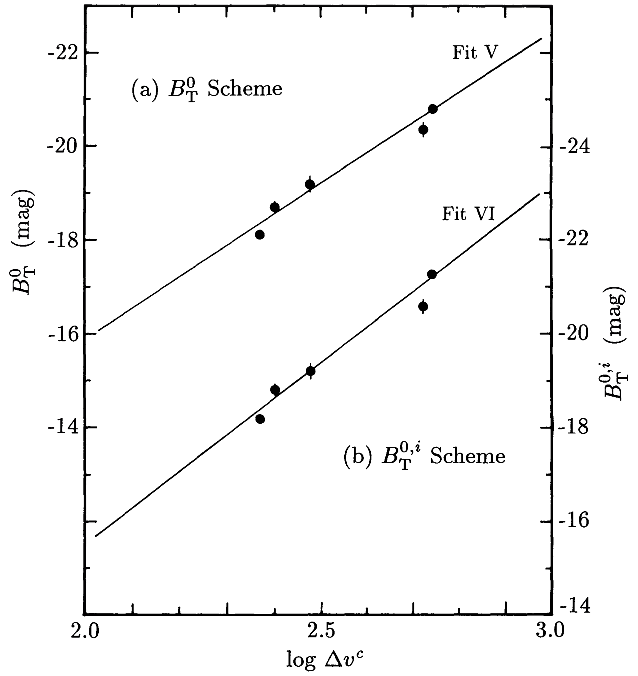

FIG. 7.—Same as Fig. 6 with the Freedman's distance scale for local calibrators.

with the form

$$-M_{B_T^0} = A + B\,(\log \Delta v^c - 2.5)\,, \qquad (4)$$

is given for both magnitude correction schemes in Table 5, and examples of the fit are shown in Figure 6 (Fits I and II in Fig. 6*a* and Fits III and IV in Fig. 6*b*). The average values of A_B and A_i for the eight local calibrators are shown in Table 5. The slope parameter of the fit is not quite well determined and has an uncertainty as large as 0.5–1. The effect on the distance estimation, however, turns out to be quite small, because in practice, we are comparing two sets of galaxies with similar line widths. We note that the fit with the RSA scheme gives a steeper slope (by ~ 1 unit compared to that with the RC2 scheme), and a larger intercept. This makes the total magnitude $M_{B_T^{0,i}}$ of the local calibrators 0.3 mag brighter than $M_{B_T^0}$ at $\log \Delta v^c = 2.6$. The difference in the two total magnitude schemes, however, to a large extent cancels between the local calibrators and the Coma galaxies, so that the net effect on distance estimations is small as we see in § 3.3 below.

A similar fitting is also made using Freedman's distances[6] (Freedman 1990) for five galaxies (M31, 24.4 ± 0.1; M33, 24.5 ± 0.2; NGC 300, 26.5 ± 0.2; NGC 2403, 27.5 ± 0.3 and M81, 27.6 ± 0.3) with the given dispersions (plus photometry errors) as input errors of the chi-square fitting (Fits V and VI; see Fig. 7). The resulting chi-square is impressively small with given small input errors. The fits lead to a result about 0.08 mag brighter for the local calibrators. We note, however, that her assumed distance to the LMC (her zero point) may be subject to an uncertainty of ± 0.07 mag. Our final remark is that de Vaucouleurs distance (de Vaucouleurs 1978a, b) for the eight galaxies in Table 4 would yield zero points about 0.2 mag smaller than is the case with Tammann's (1987) calibrators.

In this paper we adopt Fit I as our reference choice.

[6] Freedman used $(m - M)^0 = 18.5$ for the LMC, in agreement with the value in Tammann (1987).

3.2. *Tully-Fisher Relation and the Distance to the Coma Cluster*

A few selection procedures are needed prior to obtaining the TF relation for galaxies in the Coma cluster. We first select out the galaxies in the foreground and background fields. Using the guide curve for membership as a function of line-of-sight velocity, v, and the angular distance, θ, from the cluster center given by Kent & Gunn (1982), we take galaxies which satisfy (this corresponds to 2.5 σ_v with σ_v the rms velocity dispersion

TABLE 5

TULLY-FISHER PARAMETERS FOR THE LOCAL CALIBRATORS

Fit Number	Number of Calibrators	Correction Scheme	Distance Moduli	A	B	χ^2
I	8	B_T^0	KCT/T	19.12 ± 0.16	6.35 ± 0.86	4.5
II	14	B_T^0	KCT/T	19.16 ± 0.15	5.92 ± 0.68	4.6
III	8	$B_T^{0,i}$	KCT/T	19.29 ± 0.16	7.50 ± 0.86	3.3
IV	14	$B_T^{0,i}$	KCT/T	19.34 ± 0.15	7.04 ± 0.68	4.0
V	5	B_T^0	Freedman	19.18 ± 0.10	6.56 ± 0.48	2.9
VI	5	$B_T^{0,i}$	Freedman	19.36 ± 0.10	7.64 ± 0.48	4.4

at a given angular distance)

$$4825 \text{ km s}^{-1} < v < 9075 \text{ km s}^{-1} \quad \text{for } \theta < 1°$$
$$5400 < v < 8500 \quad \text{for } 1° < \theta < 2°$$
$$5775 < v < 8125 \quad \text{for } 2° < \theta < 3°$$
$$5875 < v < 8025 \quad \text{for } 3° < \theta < 4.°3$$

as member of the Coma cluster. We are then left with 42 galaxies for the Coma cluster member.

The selection for inclination (i) is somewhat arbitrary. The necessity to make a cut in i results not only to suppress an unreasonably large correction by the $(\sin i)^{-1}$ factor and to suppress the effect of the turbulence contribution on the line width, but also to alleviate the uncertainty in the inclinations that orginate from errors in b/a. In order to constrain the error of Δv^c data below 10% level ($\Delta m < 0.2$ mag) given a 10% uncertainty in b/a, we have to impose the cut $i \geq 45°$. On the other hand, we cannot impose a stronger selection criterion to the present sample if we are to keep the sample size reasonable. Therefore we used the cut $i > 45°$ as a compromise. This leaves 30 galaxies as indicated in Table 3. The average values of the absorption correction parameters are given in Table 6.

Figure 8*a* presents the TF relation for the Coma cluster with the B_T^0 scheme. If we fit the data with

$$B_T^0 = a - B(\log \Delta v^c - 2.5) , \quad (5)$$

where $B = 6.35$, we obtain $a = 14.95 \pm 0.08$ with the (nominal) dispersion $\sigma = 0.47$. This leads to the nominal distance modulus $(m - M)^0_{\text{Coma}} = 34.07$ using Fit I in Table 5. If we adopt the $B_T^{0,i}$ scheme, we obtain $a = 14.87 \pm 0.10$ ($\sigma = 0.55$) with B fixed to be 7.50 (Fit III), or the modulus $(m - M)^{0,i}_{\text{Coma}} = 34.16$. The fit is shown in Figure 8*b*. The dispersion is slightly larger with the $B_T^{0,i}$ scheme. Both distance moduli increase by 0.08 mag, if Friedman's (1990) distances are used for the local calibrators.

3.3. *Estimate of Uncertainties and the Intrinsic Dispersion of the TF Relation*

We summarize in Table 7 uncertainties in the distance modulus and their sources. Most of the sources of uncertainties in the input data were discussed in the preceding sections. We present random errors (we divided the dispersion by the square root of the number of samples where they are of statistical nature) and possible biases separately. The total uncertainty from random errors is estimated by quadrature. Biases are arithmetically added to estimate the total amount.

We note that large uncertainties in the absorption corrections tend to cancel between the Coma galaxies and the local calibrators. As seen in Table 6, the difference in the Galactic extinction correction $\langle A_B(\text{Coma}) - A_B(\text{l.c.})\rangle$ is -0.09 (RC2), -0.07 (RSA) and -0.08 (BH) for the three schemes. In this quantity a substantial zero point error in A_B cancels. A similar

TABLE 6

AVERAGE VALUES OF THE ABSORPTION CORRECTION FOR THE EIGHT LOCAL CALIBRATORS AND THE 30 COMA GALAXIES

	LOCAL CALIBRATORS			COMA GALAXIES		
AVERAGE	RC2	BH	RSA	RC2	BH	RSA
$\langle A_B\rangle$	0.28	0.12	0.07	0.19	0.04	0
$\langle A_i\rangle$	0.23	...	0.59	0.29	...	0.67

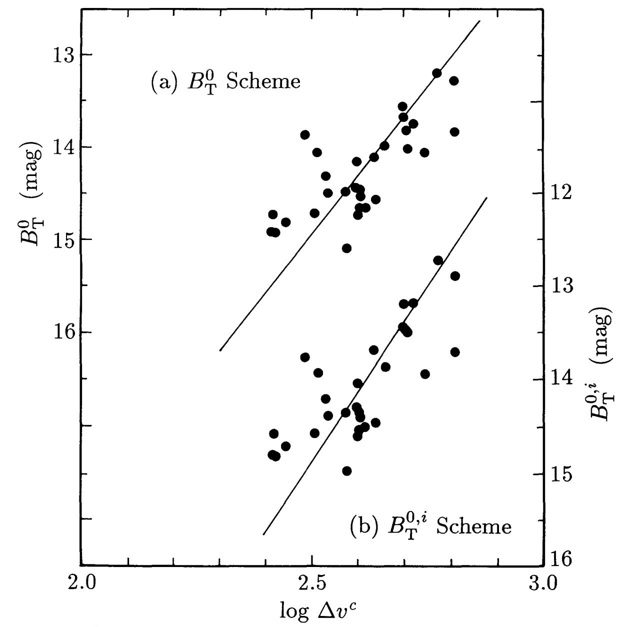

FIG. 8.—(*a*) TF relation for 30 galaxies in the Coma cluster. The curve is obtained by the least-square fit with the slope fixed to be $B = 6.35$. The B_T^0 scheme is adopted. (*b*) Same as (*a*) with the $B_T^{0,i}$ scheme.

cancellation also appears in the internal absorption correction; $\langle A_i(\text{Coma}) - A_i(\text{l.c.})\rangle$ only varies from $+0.06$ (RC2) to $+0.08$ (RSA) in spite of a large uncertainty in A_i for individual galaxies. We may allocate the net error of 0.02 to the Galactic extinction, and 0.04 (the difference doubled) to the internal absorption. The uncertainty caused by the absorption correction, which has been claimed to be a disadvantage of using B-band photometry, is much smaller than one naively expects from the values of A_B and A_i themselves.

We estimate uncertainties in the distance modulus caused by those in b/a by assuming that galaxies are distributed in a spatially random manner. We find that 10% rms error in b/a leads to a dispersion of 0.18 mag if the cut $i > 45°$ is imposed. We note that this value increases to 0.30 mag, if this cut is loosened to be $i > 35°$.

It is not easy to estimate the intrinsic dispersion of the TF relation. The dispersion σ which we obtained above is a sum of the intrinsic scatter and scatter arising from errors of observations as well as of various corrections for individual galaxies. This dispersion may also receive a contribution from the sample incompleteness bias. To study this point we give in Figure 9 the scatter around the fitted line (5) in the form of histograms. The curve shows the Gaussian distribution. In the same figure we also show the scatter for $\log \Delta v^c > 2.6$ (*hatched region*) which receives little sample incompleteness bias (discussed below). We see that the dispersion is substantially reduced ($\sigma = 0.26$ mag) and the central value is shifted above by $\Delta m = 0.25$ mag. This suggests that the true dispersion (including errors of observation) could be as small as $\sigma = 0.26$ mag. Due to the paucity of galaxies with $\log \Delta v^c > 2.6$, however, we conclude conservatively that the dispersion is somewhere between $\sigma = 0.26$ mag and 0.47 mag. Since the uncertainty in the line width (measurements and inclination corrections) and in intrinsic absorption corrections may also contribute to the dispersion on the order of 0.2 mag, we may presume that the intrinsic scatter is less than the above values.

TABLE 7

UNCERTAINTIES FOR THE DISTANCE MODULUS TO THE COMA CLUSTER

Item	Source of Errors	Dispersion (mag)	Errors to $(m-M)^0$: Random	Bias
	Coma Cluster Galaxies ($N = 30$)			
1	H I line width data ($\sigma_{\Delta v} \simeq 40$ km s^{-1})	0.25	0.046	...
2	Turbulent velocity corrections for $i > 45°$($\Delta v_T \lesssim 20$ km s^{-1})	...	...	[+0.12[a]]
3	Inclination corrections to the line width ($i > 45°$)			
	Errors in b/a ($\sigma_{b/a} \simeq 10\%$)	0.08	0.014[b]	...
	Inclination formula model dependence ($\Delta i \simeq 5\%$)	...	0.05	...
4	Photometry			
	Zero point	...	0.08	+0.13[c]
	Inhomogeneity of measurement and growth curve fitting	0.042	0.008	...
5	Galactic absorption correction (RC2 taken as reference)	...	...	[−0.19[d]]
6	Internal absorption correction			
	Model dependence (RC2 taken as reference)	...	...	[+0.38[e]]
	Errors in b/a ($\sigma_{b/a} \simeq 10\%$)	0.033	0.006[b]	...
7	K-correction error	0.01	0.002	...
8	Intrinsic scatter of the TF	0.40	0.073	...
9	Sample incompleteness bias corrections			
	Selection functions	...	<0.02	...
	Dispersion estimate	...	...	−0.09
	Local Calibrators ($N = 8$)			
10	Local calibrator distance	...	...	+0.08
11	Slope parameter indetermination	...	<0.02	...
12	H I line width ($\sigma_{\Delta v} \simeq 15$ km s^{-1})	0.098	0.034	...
13	Turbulent velocity corrections	...	...	[−0.12[a]]
14	Photometry	0.04	0.014	...
15	Galactic absorption correction	...	...	[+0.21[d]]
16	Internal absorption correction	...	...	[−0.36[e]]
17	Intrinsic scatter	0.40	0.14	...
	Total uncertainty	...	±0.20 (quadrature)	+0.27−0.09

NOTE.—Numbers in square brackets (tends to) cancel between the Coma galaxies and the local calibrators.

[a] Model-dependence cancels each other.

[b] Errors always appear in the additive sign.

[c] (BASMHS zero point) − (zero point of this work).

[d] Prescritpion dependence tends to cancel each other. We take 0.02 for a net error.

[e] Model-dependence tends to cancel each other. We take 0.04 for a net error.

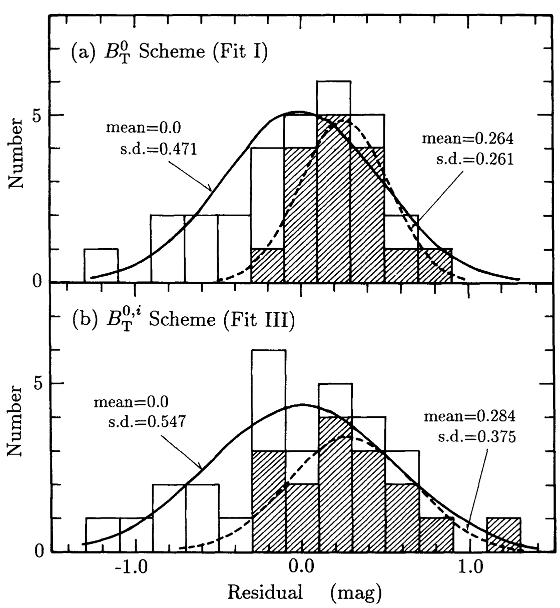

FIG. 9.—Scatter of the Tully-Fisher plot around the line (5). The hatched region shows the scatter for galaxies with log $\Delta v^c > 2.6$. Solid lines are the Gaussian curve with $\sigma = 0.47$ and 0.26 mag for (*a*) and $\sigma = 0.55$ and 0.38 mag for (*b*).

Our value for the scatter is in agreement with those quoted in Pierce & Tully (1988) and Burstein & Raychaudhury (1989), but are considerably smaller than that in KCT who reported that σ is as large as 0.7 mag. To estimate the total uncertainty in Table 7 we adopt an intrinsic scatter of $\sigma = 0.4$ mag as a rather conservative estimate. (We also assume the same value of σ for local calibrators to estimate the error of the fit. The value thus obtained virtually agrees with the error of A given in Table 5.)

The total uncertainty that we obtained is $\Delta(m - M) = \pm 0.20$ (random error) + 0.21/ − 0.00 (bias) (excluding items 5, 6, 9, 15, and 16 in Table 7 which we treat separately). Half of the random error arises from indetermination of the local distance scale (0.15 mag).

3.4. *Cluster Population Incompleteness Bias*

The fact that galaxies with a smaller H I line width tend to lie above the curve of equation (5) indicates the existence of the population incompleteness bias in the nominal estimate of the distance. To examine this point more clearly we plot in Figure 10 the "distance modulus" of each galaxy calculated with the TF relation as a function of the line width. We see an appreciable increase of the modulus towards the brighter end. We then estimate the correction for the population incompleteness bias in the following way. The bias on the distance modulus μ

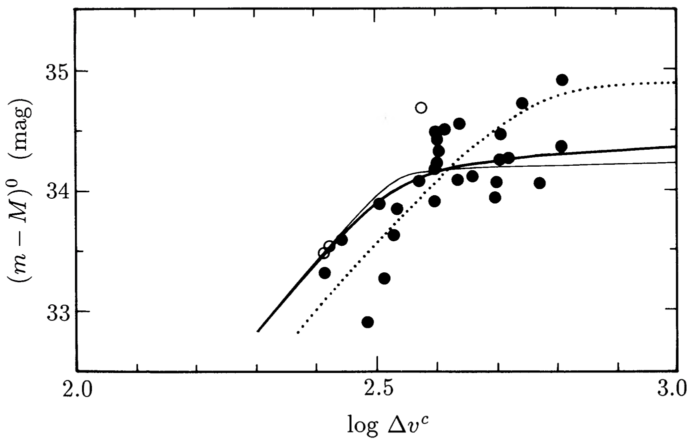

FIG. 10.—"Distance modulus" obtained for each galaxy as a function of the H I line width. Solid curves are the best-fits expected for $\sigma = 0.4$ mag (*thick line*) and 0.25 mag (*thin line*) calculated with the selection function discussed in the text. Three galaxies denoted by open circles are those which do not satisfy $B_T^0 < 14.8$ mag and omitted from the fit. For the sake of comparison, a dotted curve is added which represents the bias that occurs when the selection function is artificially cut at $m_z = 14.5$ mag (see Fig. 3).

at a given $p = \log \Delta v$ is given by

$$\Delta\mu_p = \frac{\int_{-\infty}^{\infty} dm\, mf(m)N(m, p)}{\int_{-\infty}^{\infty} dm\, f(m)N(m, p)} - \frac{\int_{-\infty}^{\infty} dm\, mN(m, p)}{\int_{-\infty}^{\infty} dm\, N(m, p)}\,, \quad (6)$$

where $f(m)$ is the selection function for the sample, and $N(m, p)$ is the number of galaxies in the interval of $(m - m + dm, p - p + dp)$ and it is assumed to be

$$N(m, p)dm\,dp = \phi(m)(2\pi)^{1/2}\sigma_p e^{-[p-p(m)]^2/2\sigma_p^2}\,, \quad (7)$$

following Teerikorpi (1984, 1987). For the luminosity function $\phi(m)$ $(m = \mu - M)$ we take the Schechter form

$$\phi(L)dL = \phi^*(L/L^*)^{\alpha} e^{-L/L^*} dL/L^* \quad (8)$$

with L^* corresponding to $M^* = -19.5$ mag and $\alpha = -1.1$. The result of our calculation is quite insensitive to the details of the luminosity function. We set the dispersion (intrinsic scatter plus scatter by errors in the input) to be $\sigma_p = \sigma/B$ with B the slope of the TF relation.

The selection function f is estimated from Figure 3, and the form used in this work is also shown in the same figure. Though the estimate of the selection function is ambiguous for brighter magnitudes, the final result depends little on the choice of f for the brighter part. We imposed a sharp cutoff $f = 0$ for $m_z > 15.5$ mag as the result is sensitive to the tail of the fainter end.[7] We then translate this selection function into the one in the B_T^0 scheme by $B_T^0 = m_z - 0.19 - \langle A_B(\text{Coma})\rangle - \langle A_i(\text{Coma})\rangle$. The limiting magnitude $m_z = 15.5$ mag corresponds to $B_T^0 = 14.8$ mag.

We have made a least-square fit with the curve predicted by equation (6) to the data of Figure 8 by varying the distance modulus $\mu^0 = (m - M)^0$. In this procedure we removed three galaxies which do not satisfy $B_T^0 \leq 14.8$ for consistency (denoted by open circles in Fig. 8). The two curves corresponds to $\sigma = 0.4$ and 0.25 mag. The resulting μ^0 represent our best estimate for the true distance modulus to the Coma cluster. We obtain $\mu^0 = 34.34$ for $\sigma = 0.4$ mag and 34.25 for $\sigma = 0.25$ mag. From these values we may conclude

$$\mu^0 = 34.34 \pm 0.20^{+0.21}_{-0.09} \quad (9)$$

for the B_T^0 scheme. A similar analysis with the $B_T^{0,i}$ scheme leads to

$$\mu^{0,i} = 34.49 \pm 0.20^{+0.21}_{-0.09}\,. \quad (10)$$

The error attached includes both the error of the fit and the uncertainties discussed above. As seen in Figure 10 we detect very little sample incompleteness bias for $\log \Delta v^c > 2.6 (B_T^0 < 14.2$ mag), once the limiting magnitude is as deep as $m_z = 15.5$ mag. For the sake of comparison we show in the same figure a dotted curve which indicates that a sample incompleteness bias as large as 0.7 mag could result, only if the limiting magnitude were as shallow as $m_z = 14.5$ mag.

4. DISCUSSION

4.1. *Analysis with a Sample of 11 Galaxies Used by* ABMHSC

In order to compare with other work we repeated our analysis with a sample of a reduced size. We select 11 galaxies (IC 842, 4088, NGC 4966, 5081, UGC 7978, 8013, 8017, 8161, 8195, 8244, Z160058) which are in the analysis of ABMHSC. [They used 13 galaxies, one of which (UGC 7750) is outside our 260′ circle, and another (Z130008; $i = 44°$) is dropped from our sample because of the inclination cut.] The galaxies contained in this reduced sample are marked by solid circles in Figure 11. This figure demonstrates that this reduced sample looks as if the galaxies are almost randomly chosen from the full sample, and that the sample is not strongly biased as presumed in KCT.

We present in Table 8 the result of our analysis. The distance

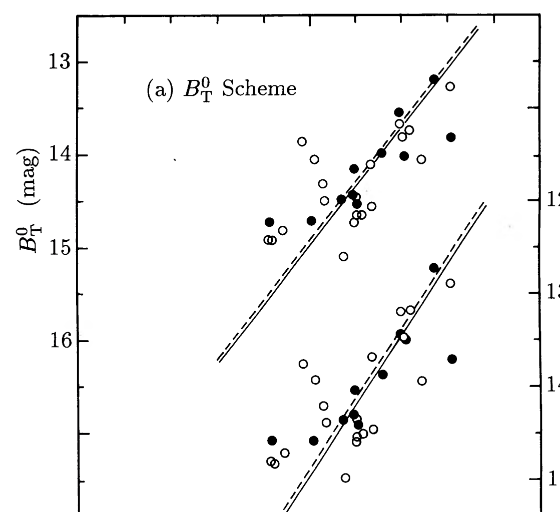

FIG. 11.—Tully-Fisher relation for a subsample. The 11 galaxies used in ABMHSC are denoted by solid circles. The solid line is the best-fit for this subsample and dashed line shows the TF plot for the full sample for comparison.

[7] The result, however, is only weakly sensitive to the completeness fraction at the faintest magnitude. Taking account of the fact that the completeness of the CGCG might be suspect close to its limiting magnitude, we checked the resulting bias by varying $f(15 \leq m_z \leq 15.5$ mag) by a factor of 1/2–2. For such a change the incompleteness bias correction to the distance modulus would change within the range of ± 0.05 mag.

TABLE 8

Tully-Fisher Analysis Using Subsamples

Photometry	A_B	A_i	m(Coma) at log $\Delta v^c = 2.6$	M(l.c.) at log $\Delta v^c = 2.6$	Distance Modulus (Nominal)
			Full Sample		
Kiso	RC2	RC2	14.31	−19.76	34.07
Kiso	BH	RC2	14.46	−19.61	34.06
Kiso	RSA	RSA	14.12	−20.04	34.16
			Subsample (11 Galaxies)		
Kiso	RC2	RC2	14.34	−19.76	34.10
			Subsample (10 Galaxies)		
BASMHS	RC2	RC2	14.64	−19.76	34.40
BASMHS	BASMHS	BASMHS	14.79	−19.58[a]	34.37
BASMHS	BASMHS (with local calibrator distances by ABMHSC)	BASMHS	14.79	−19.57[a]	34.36

[a] M31, M33, and NGC 2408 are used as local calibrators.

moduli shown in this table represent our nominal values without the correction for sample incompleteness. The first three rows are results of our full sample discussed in § 3. We also included analyses using the B-band photometry of BASMHS which has been used in all previous TF analyses for the Coma cluster (they did not give the B-band photometry data for UGC 8195, and hence we used 10 galaxies for this analysis) as well as their absorption correction scheme.

We see that the result derived from the reduced sample differs very little ($\Delta\mu^0 = +0.03$ mag) from that with the full sample. Our second remark is that the difference of 0.27 mag seen between row 4 and row 6 is ascribed to -0.03 in A_B plus A_i, and $\sim +0.3$ in the photometry (0.13 zero point plus $\sim$0.15 growth curve fitting).

4.2. *Comparison with Other Tully-Fisher Analyses*

First, Aaronson et al. (ABMHSC) derived $\mu = 34.5 \pm 0.1$ from the H band TF relation for the 13 galaxies mentioned above. They did not present the B-band TF analysis. The difference of their value and ours (0.4 mag) is not ascribed to the difference in the samples (<0.1 mag), nor to the local calibrator distances (0.04 mag). Most of the difference is to be ascribed to the photometry.

We made the B-band TF analysis using their photometry data and their absorption correction scheme (BASMHS) for the sample of 10 galaxies discussed above (row 6 of Table 8). We obtained $\mu = 34.37$, if we adopted the three local calibrators (M31, M33, and NGC 2403) used by ABMHSC. Most of the difference between this case and our results from that arises in the B-band photometry.

Second, Bottinelli et al. (1987) used 24 galaxies (including 13 of the ABMHSC sample). Of them, 14 are in our final sample. Their analysis using the B_T^0 scheme gives $(m - M)^0 = 33.8$ (with the use of the de Vaucouleurs 1978a, b calibrators) with a dispersion of $\sigma = 0.89$. The scatter of their TF plot is considerably larger than ours. This large scatter is ascribed to inclusion of galaxies, the cluster membership of which is not certain (e.g., NGC 4921, Zw 160076 and Zw 159090; these galaxies do not satisfy the membership criterion taken in the present work), and to a loose cut for the inclination ($i > 35°$; $\frac{1}{4}$ of the galaxies in their sample have inclinations $35° < i < 45°$). Their miscorrection of the photometric data for two galaxies (NGC 5065, UGC 8195, for which BASMHS did not present B-band photometry data) also contributed to the increase of the dispersion. The sample incompleteness effect is not apparent in their figure, perhaps due to this large scatter. They have suggested, however, that 12 galaxies with $B_T < 14.6$ mag be used to avoid incompleteness bias in the estimate of the Coma cluster distance, which leads to 33.9 with $\sigma = 0.78$. There remains a large scatter also after this selection by the reason described above. The quality of the sample that they used seems too poor for an accurate determination of the distance to the Coma cluster.

Finally, Kraan-Korteweg et al. (KCT) used 12 galaxies (the ABMHSC sample). [In their B-band TF analysis, the magnitude for UGC 8195, which consists of a singular data point in their figure (Fig. 8), is inherently in error by more than 1 mag.] The nominal distance modulus derived from their figure is $\sim$34.5 (with the $B_T^{0,i}$ scheme). This value lies within our allowed range and the difference between this and our reference value is attributed to the photometry ($\sim$0.3), the correction scheme ($\sim$0.1) and the local calibrator distances ($\sim$0.1). KCT have conjectured a very large sample incompleteness bias in the data and proposed a 2 σ upper envelope fit to estimate the true distance modulus, giving $m - M = 35.5$. When we increased the sample size by a factor of 2.5 (the increased sample is reasonably complete to $m_z = 14.5$ mag, and completeness is under control down to $m_z = 15.5$), however, we find that the new data fall in the region where the previous 13 data points are distributed. Our analysis indicates that the bias is not as strong as KCT suggested, and the "2 σ upper envelope prescription" leads to an incorrect answer.

4.3. *Consistency with the Virgo Distance*

The difference of the distance moduli between the Coma and Virgo clusters has been studied by a number of authors with the use of a variety of distance indicators. We quote here some of the results with relatively well-established distance indicators; i.e., $(m - M)^0_{\text{Coma-Virgo}} = 3.69$ (infrared TF relation by ABMHSC), 3.65 (D_n–σ relation by Dressler et al. 1987b) and 3.75 (Type Ia supernovae by Capaccioli et al. 1990). If we combine these values with our modulus to the Coma cluster, we obtain $(m - M)^0_{\text{Virgo}} = 30.65$–$30.75$, or the distance of 13.5–14.1 Mpc. This value is consistent with the so-called "short distance scale" to the Virgo cluster, examples of which are given by 15.6 ± 1.5 Mpc (Pierce & Tully 1988), 12.8–19.4 Mpc (Pierce 1989), 14 ± 1.4 Mpc (Tonry, Ajhar, & Luppino 1990), 14.7 ± 1.0 Mpc (Jacoby, Ciardullo, & Ford 1990).

5. CONCLUSION

We have made an estimate of the distance to the Coma cluster using the *B*-band Tully-Fisher relation. We took all galaxies, for which H I line width data are available, in a circle of 260′ radius centered on the Coma cluster and obtained surface photometry for these 48 candidate galaxies. The sample is reasonably complete to $m_Z = 14.5$ mag for late-type galaxies and represents a significant fraction down to $m_Z = 15.5$ mag. We estimated the sample incompleteness bias on the distance estimate. We also made a careful analysis of the uncertainties in each step of the determination of the distance by the TF relation.

The 30 galaxies with inclinations $i > 45°$ are used as a final sample to estimate the distance modulus to the Coma cluster. Averaging the values in equations (9) and (10) for the two different absorption correction schemes, we obtain $(m - M)^0_{\rm Coma} = 34.41$. If we take into account the zero point error of the photometry, we obtain our final result

$$(m - M)^0_{\rm Coma} = 34.48 \pm 0.20^{+0.22}_{-0.23} \text{ mag} ,$$

where the value includes the sample incompleteness bias correction of $\sim$0.3 mag and the error includes all uncertainties ($\pm$0.2 mag for random errors and $^{+0.22}_{-0.23}$ mag for possible systematic biases) of the input data. The analysis shows that our sample suffers from an appreciable sample incompleteness bias, but that it cannot be as large as 1.0 mag as suggested by KCT. We conclude that a distance modulus of 35.0 is quite a marginal value, once we accept the validity of the Tully-Fisher relation independent of possible environmental effects.

We have shown that the intrinsic scatter of the *B*-band Tully-Fisher relation is smaller than 0.4 mag, and it could be as small as 0.25 mag.

The estimate of the average recession velocity for the Coma cluster does not differ by more than 1% among different estimators: Rood et al. (1972) gave the value $v_0 = 6888$ km s^{-1} after the correction to the centroid of the local group $+300 \sin l \cos b$ km s^{-1} from the heliocentric velocity. Tifft & Gregory (1976) reported $v_0 = 6952$ km s^{-1}. ABMHSC and Dressler et al. (1987b) took 6931 and 6890 km s^{-1}, respectively. Here we adopt $v_0 = 6925$ km s^{-1} obtained from the most comprehensive catalog of Kent & Gunn (1982) with their membership criterion. (We remark that the average of the velocity over the 42 Coma cluster member galaxies of our sample is 6967 km s^{-1} consistent with the values quoted here.) If we correct for the Virgocentric infall with a velocity of 300 ± 100 km s^{-1}, we obtain the true Hubble expansion velocity of 7210 km s^{-1} for the Coma cluster. Our distance modulus then leads to the Hubble constant of

$$H_0 = 92^{+21}_{-17} \text{ km s}^{-1} \text{ Mpc}^{-1} .$$

One of us (M. F.) would like to thank John Bahcall for his hospitality at the Institute for Advanced Study, Princeton, where this work was initiated. We wish to thank Walter Saurer for his help in the photometry data reduction. We are indebted to Gregory Bothun for his valuable comments on photometry. This work was supported in part by Grant-in-Aid of the Ministry of Education No. 02211207 (Japan) at the Kyoto University and by NSF Grants Nos. PHY-8620266 (M. F.) and AST-8513087 (H. J. R.) at the Institute of Advanced Study in Princeton.

REFERENCES

Arp, H. 1988, A&A, 202, 70
Aaronson, M., Bothun, G., Mould, J., Huchra, J., Schommer, R. A., & Cornell, M. E. 1986, ApJ, 302, 536 (ABMHSC)
Aaronson, M., Huchra, J., & Mould, J. 1979, ApJ, 229, 1
Aaronson, M., Mould, J., & Huchra, J. 1980, ApJ, 237, 655
Aaronson, M., Mould, J., Huchra, J., Sullivan II, W. T., Schommer, R. A., & Bothun, G. D. 1980, ApJ, 239, 12
Aaronson, M., et al. 1982, ApJS, 50, 241
Bothun, G. D., Aaronson, M., Schommer, B., Mould, J., Huchra, J., & Sullivan III, W. T. 1985, ApJS, 57, 423 (BASMHS)
Bottinelli, L., Fouqué, P., Gouguenheim, L., Paturel, G., & Teerikorpi, P. 1987, A&A, 181, 1
Bottinelli, L., Gouguenheim, L., Paturel, G., & de Vaucouleurs, G. 1983, A&A, 118, 4
Burstein, D., & Heiles, C. 1978, ApJ, 225, 40
———. 1984, ApJS, 54, 33 (BH)
Burstein, D., & Raychaudhury, S. 1989, ApJ, 343, 18
Capaccioli, M., Cappellaro, E., Della Valle, M., D'Onofrio, M., Rosino, L., & Turatto, M. 1990, ApJ, 350, 110
Chincarini, G. L., Giovanelli, R., & Haynes, M. P. 1983, ApJ, 269, 13
Cornell, M. E., Aaronson, M., Bothun, G., & Mould, J. 1987, ApJS, 64, 507
Davis, M., & Peebles, P. J. E. 1983, ARA&A, 21, 109
de Vaucouleurs, G. 1977, ApJS, 33, 211
———. 1978a, ApJ, 223, 730
———. 1978b, ApJ, 224, 710
———. 1982, ApJ, 253, 520
de Vaucouleurs, G., & Corwin, Jr., H. G. 1977, ApJS, 33, 219
de Vaucouleurs, G., de Vaucouleurs, A., & Corwin, Jr., H. G. 1976, Second Reference Catalogue of Bright Galaxies (Austin: University of Texas Press) (RC2)
Dressler, A., Faber, S. M., Burstein, D., Davies, R. L., Lynden-Bell, D., Terlevich, R. J., & Wegner, G. 1987a, ApJ, 313, L37
Dressler, A., Lynden-Bell, D., Burstein, D., Davies, R. L., Faber, S. M., Terlevich, R. J., & Wegner, G. 1987b, ApJ, 313, 42
Feast, M. W. 1987, Observatory, 107, 185
Fouqué, P., Bottinelli, L., Gouguenheim, L., & Paturel, G. 1990, ApJ, 349, 1
Freedman, W. L. 1990, ApJ, 335, L35
Haynes, M., & Giovanelli, R. 1984, AJ, 89, 758
Hubble, E. P. 1926, ApJ, 64, 321
Huchra, J. P. 1985, in The Virgo Cluster of Galaxies, ed. O.-G. Richter & B. Binggeli (Garching: ESO), 181
Huchtmeier, W. K., Richter, O.-G., Bohnenstengel, H. D., & Hauschildt, M. 1983, ESO Rept. No. 250, unpublished
Jacoby, G. H., Ciardullo, R., & Ford, H. C. 1990, ApJ, 356, 332
Jacoby, G. H., Ciardullo, R., Ford, H. C., & Booth, J. 1989, ApJ, 334, 704
Kent, S. M., & Gunn, J. E. 1982, AJ, 87, 945
Kraan-Korteweg, R. C., Cameron, L. M., & Tammann, G. A. 1988, ApJ, 331, 620 (KCT)
Lewis, B. M. 1983, AJ, 88, 962.
———. 1987, Observatory, 107, 201
Longo, G., & de Vaucouleurs, A. 1984, University of Texas Monograph in Astronomy, No. 3
Madore, B. F., Welch, D. L., McAlary, C. W., & McLaren, R. A. 1987, ApJ, 320, 26
Nilson, P. 1973, Uppsala General Catalogue of Galaxies, Acta Uppsala Univ., Ser. V:A, Vol. 1 (UGC)
Okamura, S. 1988, PASP, 100, 524
Pierce, M. J. 1989, ApJ, 344, L57
Pierce, M. J., & Tully, R. B. 1988, ApJ, 330, 579
Richter, O.-G., & Huchtmeier, W. K. 1984, A&A, 132, 253
Rogstad, D. H., Crutcher, R. M., & Chu, K. 1979, ApJ, 229, 509
Rood, H. J., Page, T., Kinter, E., & King, T. 1972, ApJ, 175, 627
Sandage, A. 1988, ApJ, 331, 605
Sandage, A., & Tammann, G. A. 1976, ApJ, 210, 7
———. 1981, A Revised Shapley-Ames Catalog of Bright Galaxies (Washington: Carnegie Institution) (RSA)
———. 1984, Nature, 307, 326
Tammann, G. A. 1987, in IAU Symposium 124, Observational Cosmology, ed. A. Hewitt, et al. (Dordrecht: Reidel), 151
Tammann, G. A., & Sandage, A. 1985, ApJ, 294, 81
Tammann, G. A., Sandage, A., & Yahil, A. 1980, in Physical Cosmology, ed. R. Balian, et al. (Amsterdam: North Holland), 53

Teerikorpi, P. 1984, A&A, 141, 407
———. 1987, A&A, 173, 39
Tifft, W. G., & Gregory, S. A. 1976, ApJ, 205, 696
Tonry, J. L., Ajhar, E. A., & Luppino, G. A. 1990, ApJ, 346, L57
Tully, R. B. 1988, Nature, 334, 209
Tully, R. B., & Fisher, J. R. 1977, A&A, 54, 661
Tully, R. B., & Fouqué, P. 1985, ApJS, 58, 67
van der Kruit, P. C., & Shostak, G. S. 1982, A&A, 105, 351
Visvanathan, N. 1989, ApJ, 346, 629
Welch, D. L., McAlary, C. W., McLaren, R. A., & Madore, B. F. 1986, ApJ, 305, 583
Williams, B. A., & Rood, H. J. 1988, private communication
Zwicky, F., Herzog, E., Wild, P., Karpowicz, M., & Kowal, C. T. 1961–1968, Catalogue of Galaxies and of Clusters of Galaxies (Zürich: L. Speich) (CGCG)